*www.maajournal.com*

*Mediterranean Archaeology and Archaeometry*
*Vol. 20, No 2, (2020), pp. 97-111*
*Open Access. Online & Print.*

**DOI: 10.5281/zenodo.3819595**

# NEW SPECTROSCOPIC DATA ON “MARMI MISCHI” BAROQUE GLASS DECORATIONS FROM “PALLIUM ALTARIS” OF MESSINA (SICILY, ITALY)

**Di Bella M.[1], Sabatino G.[2*], Giuliano A.[3], Italiano F.[1], S. Quartieri[2$], M. Triscari[2$], S. Magazù[2], A. Tripodo[2]**

*[1]Istituto Nazionale di Geofisica e Vulcanologia (INGV), Sezione di Palermo, Via Ugo La Malfa 153, 90146*
*Palermo and Sede Operativa di Milazzo, Via dei Mille 46, 98057, Milazzo (ME), Italy*
*[2]Dipartimento di Scienze Matematiche e Informatiche, Scienze Fisiche e Scienze della Terra (MIFT),*
*Università di Messina, V. Stagno d’Alcontres 31, 98166 Messina S. Agata, Italy*
*[3]Museo Regionale di Messina, Viale della Libertà, 465, 98121 Messina (ME), Italy*
[$] now retired

**Received: 24/01/2020**
**Accepted: 07/05/2020**

**Corresponding author: gsabatino@unime.it*

## ABSTRACT

The “Marmi Mischi” (mixed glass mosaic tesserae) are artificial calcium-rich glass decorations, typically used in southern Italy and Sicily during the Baroque period (1600-1700) to decorate walls and altars of religious edifices. In this study, we provide new archaeometric information on the raw materials, pigments and opacifying agents used to produce “Marmi Mischi” of “Pallium altaris” from the Messina Regional Museum. To reach this objective, all the studied glass decorations were analysed by means of non-destructive portable X-ray fluorescence (pXRF). Some of the decorations were further subjected to Environmental scanning electron microscopy (ESEM) and X-ray powder diffraction (XRPD) in the laboratory. Two types of glasses were recognised. The first one – bluish green in colour – is a basic or slightly modified “carcara glass”, characterized by high concentrations of P. The second type – dark blue, turquoise, light turquoise and red in colour – is a “carcara glass” modified by craftsmen, containing high amounts of colouring agents (Cu, Pb, Sn, Sb). The presence of schreibersite in some of the analysed samples indicates that forming occurred in extremely reducing conditions and proves that the glasses were produced in CaO furnaces called “carcara” and used to produce lime. Moreover, our results suggest that: i) the dark blue, turquoise and bluish green nuances are as a result of $Fe^{2+}$, with minor contribution by Cu and Co; ii) the light turquoise nuance is related to $Fe^{2+}$ and $Cu^{2+}$, with minor contribution by Co; and iii) the red colour is as a result of the reduction of copper to the metallic state by Sn and Pb. Ca-antimonate ($Ca_2Sb_2O_7$) was identified as an opacifying agent for the blue glassy decorations, whereas metallic Cu was identified for the red. The overall results of the chemical and physical characterization of the “Pallium altaris” glassy decorations from the Messina Regional Museum suggest that the used raw material was “carcara glass,” to which various chemical elements were suitably added to obtain the desired nuances.

**KEYWORDS**: Sicilian Baroque, carcara glass, SEM-EDX, portable XRF, Messina

## 1. INTRODUCTION

In Italy the Baroque period began late in the 1500s. The Baroque style flourished in Sicily, especially after the devastating earthquake in 1693 (Abbate, 1997; Sola, 2015). Whole cities had to be rebuilt. Splendid churches and palaces were erected according to a style that has been termed the “Sicilian Baroque style.” The churches were often richly decorated with coloured marble and mosaic inlay called “Marmi Mischi” (Giuffrè, 1992). More precisely, “mischi” refers to flat marble inlays, which become tramischi, trabischior rabischi if elements in relief are inserted, normally in white marble, as occurs during the development of this singular technique (Sola, 2015). In fact, the inlay of coloured stones is one of the characteristics of the Sicilian Baroque (Accascina, 1963; Abbate, 1997). Specifically, the main element of the church, that is the altar, was made of a single piece of polychrome marble and was decorated with gilded volutes and garlands, often inlaid with other stones, such as lapis lazuli, agates and artificial glasses (Napoleone, 2001; Piazza, 2007; Sola, 2015). The artificial glasses are frequently referred to in local historical sources as being produced locally, and they are called “smaltini” or “pietre di carcara” (i.e., lime-kiln stones), with evident reference to their origin (Balenzano and Moresi, 2004; Artioli et al., 2009).

The “Marmi Mischi” (Hills, 1999) inlay technique was introduced in Sicily during the 17th century, after the Baroque style had been established in the Island. In general, the inlay technique appeared in Sicily around the 8th and 9th centuries, during the Arab dominations that took place in Palermo, although in the Norman churches the use of the polychrome marble became a real mosaic technique. In the following years, the interest in this technique continued to decrease, but the technique re-emerged in the 16th century due to the arrival on the island of Tuscan and Lombard marble workers, which in some way led to a new exploitation of the quarries of semi-precious stones present there. On this occasion, the Sicilian marble-makers made their own style the Baroque ideas of the time and created an inimitable artistic expression that distinguished them, abandoning the severe and refined models of the Norman monuments.

Numerous churches in Palermo, Messina, Trapani, and many other centres of Sicily began to be covered in precious polychrome marble and hard stone inlays, and gradually the manufacturers became more innovative and diversified the shops, especially those from Palermo and Messina. In the 17th century, the new style had taken root that the island "stones" became indispensable in the Baroque decoration and their exportation to Tuscany, Rome, Naples, and Genoa continued, intensifying even in the following centuries.

During the Baroque productions of the “Marmi Mischi” in Southern Italy and Sicily, most artificial glasses were classified as “smaltini” or “vetri di carcara”, a term that came from the combustion slags of limestone furnaces (Montana and Gagliardo Briuccia, 1998). As far as the production of the “Marmi mischi” is concerned, the written sources of the time seem to indicate an accidental production during the kiln firing (Mongitore, 1742; Schiavo, 1756; Artioli et al., 2009). The continuous need for adequate binders for buildings and mortars was achieved through the burning, in specific “furnaces” called “carcare,” of carbonatic rocks (such as limestone, marly limestone, and/or dolomitic limestone) good for CaO production (Fig. 1; Balenzano and Moresi, 2004).

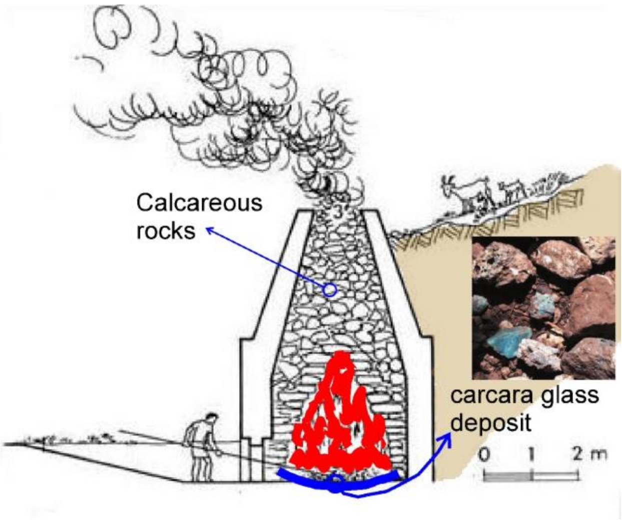

*Fig. 1 - Model of “Carcara” furnace.*

After roasting of huge quantities of these carbonates at the bottom of the furnaces, glassy to vitreous materials were found, mostly green-blue in colour (both dark and pale), which were collected and used as glasses in the "Mischi" decorations (Montana and Gagliardo Briuccia, 1998). Many pieces of these "Marmi Mischi" mosaics (frontal wall of altars, spare mosaic samples, and glassy materials in the form of cakes ready to be cut in fragments and/or slabs) are preserved at the Regional Museum of Messina (Pavone Alajmo, 2001). They are related to the Messina earthquake in 1908. This well-known seismic activity that affected over time the northeastern portion of Sicily and southern Calabria was responsible – among other damages – for impairments to the stone monumental heritage to which we also ascribe the works "Marmi Mischi" and/or the "Marble inlays".

Only Artioli et al. (2009) reported mineralogical and chemical-physical data in their study on the "smaltini di calcara", represented by blue enamels, widely used in the 17th and 18th centuries, to make altar decorations of several baroque churches in Palermo, Sicily. Their study revealed that blue smaltini represent rare ancient blue glasses pigmented by divalent iron cations, in distorted octahedral coordination, and are mixed-alkali glass accidentally produced under severely reducing conditions in the local kilns during the production of lime.

In order to improve the archaeometric knowledge on the Baroque mosaic glass decorations, we present a study of the "Marmi Mischi", commonly called "smaltini di calcara", which actually turn out to be an unusual historical case of colored glasses decorations (for a review on archaeometry, see, Liritzis et al., 2020) . In our investigation, a set of spare mosaic tesserae and glassy materials including green-blue, blue, turquoise and red glasses - recovered at the Messina Regional Museum, have been analyzed. The study aims to investigate the chemical composition and the nature of the glass matrix, colorants, and opacifying agents in all the main nuances of smaltini. The analytical approach adopted includes the mineralogical and chemical characterization of single pieces of decorations in the laboratory by scanning electron microscopy (SEM-BSE) and X-ray powder diffraction (XRPD) analyses, and the chemical characterization of altar decorations in situ using portable X-ray fluorescence (pXRF). The obtained data have been compared with those of similar glass materials of the same age acquired from some churches in Palermo and studied by Artioli et al. (2009), with the aim of garnering additional information on the used carcara raw glass.

## 2. MATERIALS AND EXPERIMENTAL METHODS

The glass decorations from the altars and walls of churches recovered at the Messina Regional Museum were provided by the Soprintendenza BB.CC. of Messina. Fig. 2 reports images of the selected and analysed samples, representative of the various colours present in the glassy decorations of the Baroque "Marmi Mischi" mosaics. The studied glassy decorations were all opaque and showed intense colouring in red, green, and several nuances of blue, from turquoise to dark blue. Two series of samples, making up a total of 40 decorations, were analysed. The first suite (PL series) included 32 decorations directly taken from the "Pallium altaris" located in a room of the Messina Museum: dark blue PL1-PL5, turquoise PL6-PL8, light turquoise PL9-PL14, bluish green PL15-PL24, red PL26-PL32. The other series was composed of erratic fragments of decorations stored in the "Fiore" deposit of the Regional Museum of Messina and belonging to similar Baroque decorations. From this second series of materials, 8 fragments of the most representative colours were selected: red (F1), turquoise (F2, F3), light turquoise (F4), dark blue (F5, F8), bluish green (F7), and one sample of carcara raw glass (F10). All the samples were analysed for major and trace elements composition (Table 1, see Appendix) by handheld XRF spectroscopy (pXRF). Moreover, samples from the "Fiore" deposit were analysed by means of Environmental Scanning Electron Microscopy (ESEM) in order to identify textures and inclusions, and X-Ray Powder Diffraction (XRPD) were performed on the opaque samples to identify crystalline phases dispersed in the glass matrix.

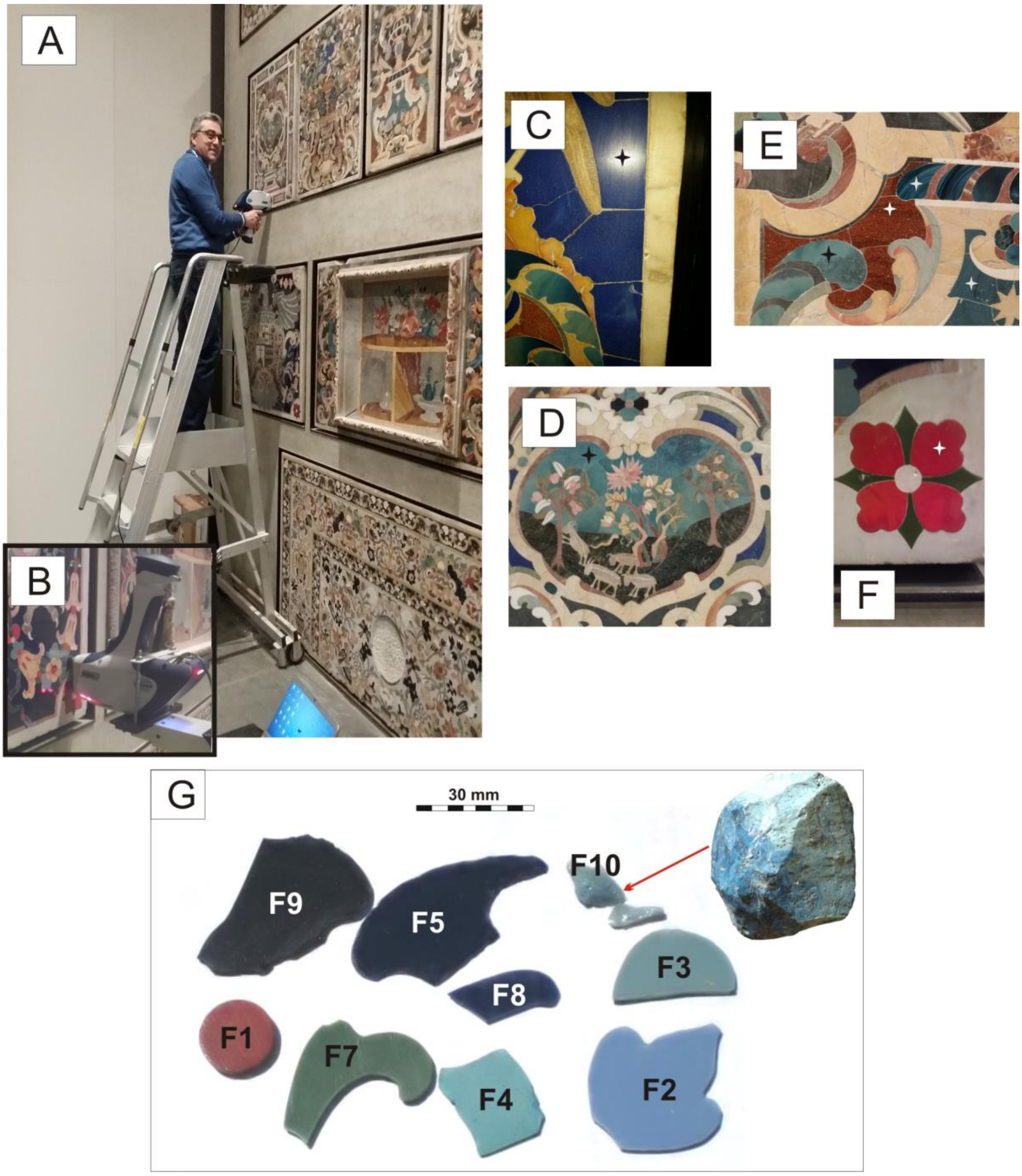

*Fig. 2 - A) The Baroque "Marmi Mischi" decorations of "Pallium altaris" kept at the Regional Museum of Messina and analysed through portable XRF; B) Particulars of the XRF analyses C) D) E) and F) Particulars of the several variously coloured analysed decorations; G) Fragments of the glassy decorations (F1-F9) and a piece of raw glass (F10) collected at the "Fiore" deposit in the Regional Museum of Messina.*

## 2.1. HANDHELD X-RAY FLUORESCENCE (XRF)

Non-destructive in situ analyses were performed using a handheld XRF S1 Titan 600 by Bruker. The TITAN 600 spectrometer (Bruker) is equipped with a silicon-drift detector FAST SDD®, with a resolution <145 eV and an analytic range from magnesium to uranium. The excitation source was a 4 W Rh target X-ray tube equipped with an automatic adjustment system that optimizes the analyses of the chemical species in terms of X-ray voltage (6 - 50 kV) and current (5 - 100 µA) values. The spot was 5 mm sized, with five-position motorized filter changer. The use of 5 filters (Ti 25 µm; Cu 200 µm + Ti 25 µm +Al 300 µm; Al 76 µm; C 60 µm, F 190 µm; no filter) is automatically managed by the instrument software on the basis of the X-ray power of the analysed elements. The nose of pXRF instrument ις in contact with the planar surface of the sample. The instrument also employs a patented X-ray geometry, namely the Sharp Beam TM Optimized Geometry (patent n. 8.223.925 by Shannon, 2012). It is a 45° angle geometry, and the beam size is controlled by a collimator that is placed between the X-ray tube and the sample. The collimator includes a plurality of ridges extending from the interior surface of the housing towards a centre of the cavity. A laptop computer was used for instrument operation and data storage. X-ray counts were processed using the S1PXRF spectra program developed by Bruker and converted to concentrations (major elements reported as oxides) using a Bruker-designed calibration program (GeoChem Trace) verified by use of standard provided by Bruker, which utilizes the Compton's scatter derived from rhodium backscatter. The GeoChem Trace is a calibration software optimized for applications in mineralogical and geochemical fields. This software includes full light element support via dual phase measurement. During pXRF analyses, the surface of the investigated object was carefully cleaned by using analytical acetone.chaeom

### 2.1.1 Environmental Scanning Electron Microscopy (ESEM)

The textural investigations of the glass matrix were mainly performed to show the presence of crystalline opacifying agents and to define their morphology; EDX analyses were run to obtain qualitative chemical analysis on these inclusions. The BSE images were obtained by an ESEM-FEI Inspect-S electron microscope coupled with an Oxford INCA PentaFETx3 EDX spectrometer, a Si(Li) detector equipped with an ultra-thin window ATW2, using a resolution of 137 eV at 5.9 keV (Mn Kα1). The energy dispersion spectral data were acquired under the following conditions: a working distance of 10 mm with an acceleration voltage of 20 kV, counting time of 60 s, count per second of approximately 3000 cps with dead time below 30%. The results were processed by INCA Energy software. This software uses the XPP matrix correction scheme developed by Pouchou and Pichoir (Pouchou and Pichoir, 1984; 1985).

### *2.1.1.1 X-Ray Powder Diffraction (XRPD)*

X-ray diffraction experiments were performed on the opaque samples to identify crystalline phases dispersed in the glass matrix. A non-destructive procedure was followed, working directly on the "smaltini" using an appropriate multi-purpose sample stage. Data were collected using a BRUKER D8 ADVANCE diffractometer with Cu Kα radiation on a Bragg–Brentano theta–theta goniometer, equipped with a SiLi solid-state detector, Sol-X. The patterns were collected from 2 to 80 2θ degrees, with a step size of 0.02° and a count time of 1 s. Observed peak positions were matched against the ICDD–JCPDS database.

## 3. DISCUSSION OF RESULTS

The obtained data are addressed to discuss, firstly, the composition of the raw glassy materials, whilst in the following paragraphs data useful for the identification of colouring and opacifying agents are discussed. Then, the obtained data related to the blue decorations are compared with those obtained by Artioli et al. (2009), a study on the Sicilian blue carcara glassy decorations from the Baroque churches of Palermo city.

### 3.1 BASE GLASS CHARACTERISTICS

The results of bulk chemistry analyses carried out with handheld XRF on all the studied samples obtained from the "Pallium altaris" (PL1-PL32) and the "Fiore" deposit (F1-F10) are reported in Table 1. The major element analysis shows that they are all silicate glasses (except for the raw glass sample F10), with silica in the range of 53 % to 79 %. The other major components vary in the following ranges: CaO from 1.4 % to 12.2 %, $Al_2O_3$ from 1.3 % to 3 %, $K_2O$ from 1.8 % to 5.4 %, and MgO from 1.8 % to 3.5 %. The high amount of $K_2O$ and MgO allowed the classification of the raw materials as plant ash to wood ash types (Fig. 3A). The variability in Ca and Mg composition could be attributed to the carbonatic rock charge, used during the production process of lime in the carcara kiln. The consistent amount of K, Na and Ca essentially derived from the plants used as fuel, given that the carbonatic rocks, e.g. limestone, are in themselves totally devoid of alkali cations (Artioli et al. 2009). The plants that are thought to be the sources of alkalis also contribute phosphorus to the glass, because the analysed carcara glass sample (F10) is P-rich, as can be observed in Tab. 1. The variation diagram of Fig. 3B shows the negative correlation between CaO and $SiO_2$. The decrease in CaO with increasing $SiO_2$, starting from the raw carcara glass to the compositions of the decorations, as can be seen in Fig. 3b, shows that silica was added to the raw materials to obtain the desired glass. Furthermore, among the major oxides, MnO (~ 0.11-0.9 %) is present as a minor component in the original raw rocks, $TiO_2$ never exceeds 0.4 %, and hence it is ascribable to impurities of oxide minerals in the raw rocks. As regards antimony oxide, it is largely used as a decolorizing and opacifying agent, and is particularly abundant in the opaque blue, low in the red, and under detection limit in the bluish green decorations (Tab. 1). Lead oxide content is very high in the opaque red decorations, F1 (PbO 52 %) and F4 (PbO 33 %), and very low in the other samples (Tab. 1).

*Tab. 1 – XRF compositional data (ppm) and the errors of the "Pallium altaris" decorations analysed in situ.*

| **Sample** | **PL1** | **PL2** | **PL3** | **PL4** | **PL5** | **PL6** | **PL7** | **PL8** | **PL9** | **PL10** | **PL11** | **PL12** |
|---|---|---|---|---|---|---|---|---|---|---|---|---|
| **Color** | **dark blue** | | | | | **turquoise** | | | **light turquoise** | | | |
| **Pigment** | **$Fe^{2+}$** | | | | | **$Fe^{2+}$** | | | **$Cu^{2+}$** | | | |
| **MgO** | < LOD | 3.2077 | 2.8145 | < LOD | < LOD | < LOD | < LOD | < LOD | < LOD | < LOD | 1.7880 | < LOD |
| **Err** | 0.0000 | 1.5006 | 1.4768 | 0.0000 | 0.0000 | 0.0000 | 0.0000 | 0.0000 | 0.0000 | 0.0000 | 1.5408 | 0.0000 |
| **$Al_2O_3$** | 0.5793 | 0.6434 | 0.9467 | < LOD | 0.8899 | < LOD | < LOD | 0.0000 | < LOD | < LOD | 0.6562 | < LOD |
| **Err** | 0.3692 | 0.3355 | 0.3424 | 0.0000 | 0.3739 | 0.0000 | 0.0000 | 0.3520 | 0.0000 | 0.0000 | 0.3448 | 0.0000 |
| **$SiO_2$** | 75.4693 | 75.3687 | 75.4194 | 76.9068 | 73.0541 | 74.7570 | 74.9750 | 74.2212 | 72.5940 | 73.9982 | 73.6595 | 71.3495 |
| **Err** | 0.6069 | 0.5785 | 0.5875 | 0.5810 | 0.5922 | 0.5840 | 0.5424 | 0.5762 | 0.4914 | 0.5072 | 0.5737 | 0.5413 |
| **$P_2O_5$** | 0.1100 | 0.1229 | 0.1314 | 0.0550 | 0.1291 | 0.0928 | 0.0609 | 0.0649 | 0.1237 | 0.1131 | 0.1548 | 0.1217 |
| **Err** | 0.0513 | 0.0465 | 0.0474 | 0.0475 | 0.0541 | 0.0525 | 0.0478 | 0.0517 | 0.0451 | 0.0446 | 0.0480 | 0.0493 |
| **$SO_3$** | 1.7031 | 0.4432 | 0.4306 | 0.8973 | 1.5522 | 5.9848 | 1.9211 | 2.1113 | 0.9584 | 0.7168 | 0.5076 | 1.0817 |
| **Err** | 0.0216 | 0.0172 | 0.0170 | 0.0199 | 0.0208 | 0.0313 | 0.0231 | 0.0230 | 0.0224 | 0.0213 | 0.0187 | 0.0217 |
| **$K_2O$** | 4.7953 | 4.1071 | 4.0641 | 3.7908 | 4.4346 | 2.1493 | 2.8617 | 2.9300 | 4.6680 | 4.6432 | 4.5893 | 2.7751 |
| **Err** | 0.0315 | 0.0284 | 0.0285 | 0.0275 | 0.0305 | 0.0222 | 0.0236 | 0.0251 | 0.0272 | 0.0275 | 0.0300 | 0.0238 |
| **CaO** | 10.9760 | 10.3303 | 10.5126 | 10.3206 | 13.8827 | 11.6255 | 12.3664 | 13.1391 | 11.0597 | 10.2618 | 9.8267 | 12.1167 |
| **Err** | 0.0451 | 0.0423 | 0.0431 | 0.0427 | 0.0501 | 0.0456 | 0.0446 | 0.0481 | 0.0401 | 0.0395 | 0.0421 | 0.0450 |
| **FeO** | 0.9543 | 0.7401 | 0.7561 | 0.7925 | 0.7778 | 0.5817 | 0.6299 | 0.6537 | 0.6797 | 0.6620 | 0.6634 | 3.5547 |
| **Err** | 0.0102 | 0.0086 | 0.0088 | 0.0089 | 0.0093 | 0.0070 | 0.0067 | 0.0073 | 0.0073 | 0.0073 | 0.0082 | 0.0175 |
| **MnO** | 0.3080 | 0.4594 | 0.4539 | 0.4255 | 0.2381 | 0.2424 | 0.3342 | 0.3535 | 0.4689 | 0.4511 | 0.4608 | 0.3986 |
| **Err** | 0.0078 | 0.0086 | 0.0087 | 0.0084 | 0.0069 | 0.0058 | 0.0062 | 0.0068 | 0.0077 | 0.0076 | 0.0087 | 0.0080 |
| **$TiO_2$** | 0.1073 | 0.0913 | 0.0905 | 0.0870 | 0.1096 | 0.0751 | 0.1003 | 0.0915 | 0.1549 | 0.1116 | 0.1102 | 0.0586 |
| **Err** | 0.0051 | 0.0049 | 0.0049 | 0.0051 | 0.0054 | 0.0050 | 0.0052 | 0.0053 | 0.0054 | 0.0052 | 0.0051 | 0.0055 |
| **NiO** | 0.1124 | 0.0904 | 0.0861 | 0.2132 | 0.0238 | 0.0404 | 0.1117 | 0.1049 | 0.0622 | 0.0595 | 0.0514 | 0.0129 |
| **Err** | 0.0028 | 0.0025 | 0.0024 | 0.0037 | 0.0015 | 0.0015 | 0.0024 | 0.0023 | 0.0025 | 0.0024 | 0.0022 | 0.0021 |
| **CoO** | 0.0674 | 0.0774 | 0.0774 | 0.0743 | 0.0094 | 0.0179 | 0.0682 | 0.0425 | 0.0283 | 0.0253 | 0.0107 | < LOD |
| **Err** | 0.0004 | 0.0006 | 0.0005 | 0.0007 | 0.0004 | 0.0004 | 0.0011 | 0.0007 | 0.0014 | 0.0012 | 0.0006 | 0.0000 |
| **CuO** | 0.0293 | 0.0453 | 0.0429 | 0.2476 | 0.0122 | 0.0576 | 0.0315 | 0.0317 | 2.4899 | 2.4487 | 2.1905 | 3.8956 |
| **Err** | 0.0015 | 0.0017 | 0.0016 | 0.0034 | 0.0011 | 0.0014 | 0.0013 | 0.0013 | 0.0095 | 0.0097 | 0.0097 | 0.0134 |
| **PbO** | 0.1349 | 0.0430 | 0.0414 | 0.0666 | 0.1333 | < LOD | 0.1246 | 0.1141 | 0.0499 | 0.0469 | 0.0375 | 0.0441 |
| **Err** | 0.0029 | 0.0022 | 0.0021 | 0.0025 | 0.0029 | 0.0000 | 0.0026 | 0.0025 | 0.0025 | 0.0024 | 0.0022 | 0.0024 |
| **$SnO_2$** | < LOD | < LOD | < LOD | < LOD | < LOD | 0.0569 | 0.0150 | < LOD | 0.0322 | < LOD | < LOD | < LOD |
| **Err** | 0.0000 | 0.0000 | 0.0000 | 0.0000 | 0.0000 | 0.0080 | 0.0075 | 0.0000 | 0.0127 | 0.0000 | 0.0000 | 0.0000 |
| **$Sb_2O_3$** | 3.2933 | 3.1710 | 3.1296 | 4.7465 | 4.0119 | 3.5269 | 5.4862 | 5.2000 | 5.7997 | 5.6772 | 4.5581 | 3.8231 |
| **Err** | 0.0175 | 0.0175 | 0.0169 | 0.0210 | 0.0192 | 0.0147 | 0.0193 | 0.0190 | 0.0229 | 0.0231 | 0.0211 | 0.0202 |
| **$As_2O$** | 0.5698 | 0.3963 | 0.3775 | 0.6067 | 0.0975 | 0.2230 | 0.4495 | 0.4432 | 0.1610 | 0.1572 | 0.1448 | 0.0186 |
| **Err** | 0.0037 | 0.0030 | 0.0028 | 0.0036 | 0.0019 | 0.0019 | 0.0027 | 0.0028 | 0.0018 | 0.0019 | 0.0019 | 0.0010 |
| **Cl** | 0.5980 | 0.6019 | 0.5762 | 0.5326 | 0.6174 | 0.5688 | 0.4041 | 0.4442 | 0.5853 | 0.5527 | 0.5325 | 0.7491 |
| **Err** | 0.0297 | 0.0267 | 0.0275 | 0.0269 | 0.0294 | 0.0279 | 0.0229 | 0.0263 | 0.0202 | 0.0211 | 0.0265 | 0.0259 |
| **Bi** | 0.2354 | 0.1831 | 0.1970 | 0.2737 | 0.0263 | < LOD | 0.0596 | 0.0540 | 0.0841 | 0.0748 | 0.0580 | < LOD |
| **Err** | 0.0038 | 0.0030 | 0.0028 | 0.0041 | 0.0022 | 0.0000 | 0.0023 | 0.0022 | 0.0029 | 0.0028 | 0.0026 | 0.0000 |

LOD – Limit of detection

**Tab. 1** – Continued.

| **Sample** | **PL13** | **PL14** | **PL15** | **PL16** | **PL17** | **PL18** | **PL19** | **PL20** | **PL21** | **PL22** | **PL23** | **PL24** |
|---|---|---|---|---|---|---|---|---|---|---|---|---|
| **Color** | **light turquoise** | | **bluish-green** | | | | | | | | | |
| **Pigment** | **$Cu^{2+}$** | | **$Fe^{2+}$** | | | | | | | | | |
| **MgO** | < LOD | < LOD | 5.3911 | 4.3647 | 5.3550 | 4.8030 | 5.7265 | 5.7237 | 5.6232 | 6.2760 | 5.8582 | 8.1146 |
| **Err** | 0.0000 | 0.0000 | 1.5227 | 1.4425 | 1.4339 | 1.4712 | 1.5706 | 1.5007 | 1.3117 | 1.4122 | 1.6441 | 1.6167 |
| **$Al_2O_3$** | < LOD | 0.5873 | 3.3894 | 3.2574 | 2.8301 | 3.2341 | 2.9431 | 2.9183 | 3.5939 | 3.6182 | 4.1190 | 3.8624 |
| **Err** | 0.0000 | 0.3652 | 0.3895 | 0.3779 | 0.3669 | 0.3818 | 0.3939 | 0.3824 | 0.3504 | 0.3674 | 0.4183 | 0.4110 |
| **$SiO_2$** | 70.6512 | 71.0846 | 67.5441 | 67.6994 | 68.4221 | 69.2820 | 68.3532 | 69.4192 | 68.7808 | 66.8229 | 66.8269 | 64.3867 |
| **Err** | 0.5388 | 0.5688 | 0.6111 | 0.5772 | 0.5856 | 0.6035 | 0.6298 | 0.6202 | 0.5344 | 0.5509 | 0.6381 | 0.6228 |
| **$P_2O_5$** | 0.1162 | 0.2067 | 1.6462 | 1.5879 | 1.7216 | 1.6093 | 1.6823 | 1.6392 | 1.2941 | 1.3685 | 1.7328 | 1.6551 |
| **Err** | 0.0481 | 0.0521 | 0.0658 | 0.0634 | 0.0638 | 0.0640 | 0.0675 | 0.0652 | 0.0553 | 0.0589 | 0.0693 | 0.0687 |
| **$SO_3$** | 0.9482 | 0.7962 | 1.5071 | 2.1664 | 1.1721 | 0.5913 | 1.1190 | 0.3329 | 0.4274 | 0.8724 | 1.1529 | 0.8576 |
| **Err** | 0.0216 | 0.0204 | 0.0170 | 0.0203 | 0.0166 | 0.0144 | 0.0153 | 0.0128 | 0.0159 | 0.0167 | 0.0156 | 0.0137 |
| **$K_2O$** | 3.7490 | 3.5774 | 5.7343 | 5.7928 | 5.7219 | 5.8508 | 5.7520 | 5.8750 | 6.1808 | 6.1315 | 6.1689 | 5.8807 |
| **Err** | 0.0269 | 0.0275 | 0.0354 | 0.0342 | 0.0341 | 0.0350 | 0.0360 | 0.0357 | 0.0329 | 0.0340 | 0.0378 | 0.0370 |
| **CaO** | 10.7235 | 12.0723 | 13.3201 | 13.5479 | 13.4264 | 13.1552 | 13.0419 | 12.7712 | 12.3846 | 13.2810 | 12.3261 | 13.5556 |
| **Err** | 0.0427 | 0.0466 | 0.0505 | 0.0490 | 0.0490 | 0.0492 | 0.0507 | 0.0493 | 0.0440 | 0.0470 | 0.0502 | 0.0522 |
| **FeO** | 3.2396 | 3.7786 | 1.0216 | 1.0198 | 0.9558 | 1.0556 | 0.9937 | 0.9574 | 1.2102 | 1.1889 | 1.3356 | 1.2687 |
| **Err** | 0.0166 | 0.0190 | 0.0111 | 0.0105 | 0.0102 | 0.0109 | 0.0111 | 0.0106 | 0.0089 | 0.0093 | 0.0113 | 0.0111 |
| **MnO** | 0.5392 | 0.5258 | 0.1213 | 0.1183 | 0.1186 | 0.1187 | 0.1164 | 0.1204 | 0.1495 | 0.1468 | 0.1516 | 0.1522 |
| **Err** | 0.0091 | 0.0094 | 0.0054 | 0.0051 | 0.0051 | 0.0052 | 0.0054 | 0.0053 | 0.0044 | 0.0046 | 0.0053 | 0.0054 |
| **$TiO_2$** | 0.0750 | 0.0738 | 0.1485 | 0.1597 | 0.1356 | 0.1544 | 0.1428 | 0.1435 | 0.2169 | 0.2080 | 0.1906 | 0.1760 |
| **Err** | 0.0055 | 0.0056 | 0.0050 | 0.0051 | 0.0049 | 0.0050 | 0.0049 | 0.0049 | 0.0052 | 0.0052 | 0.0053 | 0.0054 |
| **NiO** | 0.0493 | 0.0110 | 0.0013 | 0.0012 | 0.0000 | 0.0010 | 0.0012 | 0.0016 | 0.0017 | 0.0018 | 0.0009 | 0.0014 |
| **Err** | 0.0029 | 0.0018 | 0.0007 | 0.0008 | 0.0007 | 0.0007 | 0.0007 | 0.0007 | 0.0007 | 0.0007 | 0.0006 | 0.0006 |
| **CoO** | < LOD | < LOD | < LOD | < LOD | < LOD | < LOD | < LOD | < LOD | 0.0000 | < LOD | < LOD | < LOD |
| **Err** | 0.0000 | 0.0000 | 0.0000 | 0.0000 | 0.0000 | 0.0000 | 0.0000 | 0.0000 | 0.0005 | 0.0000 | 0.0000 | 0.0000 |
| **CuO** | 4.8057 | 2.7318 | 0.0180 | 0.0962 | 0.0080 | 0.0084 | 0.0347 | 0.0087 | 0.0082 | 0.0078 | 0.0076 | 0.0071 |
| **Err** | 0.0152 | 0.0113 | 0.0011 | 0.0021 | 0.0008 | 0.0009 | 0.0014 | 0.0009 | 0.0007 | 0.0007 | 0.0007 | 0.0007 |
| **PbO** | 0.0503 | 0.0442 | < LOD | < LOD | < LOD | < LOD | < LOD | < LOD | < LOD | 0.0017 | 0.0196 | 0.0036 |
| **Err** | 0.0026 | 0.0023 | 0.0000 | 0.0000 | 0.0000 | 0.0000 | 0.0000 | 0.0000 | 0.0000 | 0.0013 | 0.0014 | 0.0012 |
| **$SnO_2$** | < LOD | < LOD | < LOD | < LOD | < LOD | < LOD | < LOD | < LOD | < LOD | < LOD | < LOD | < LOD |
| **Err** | 0.0000 | 0.0000 | 0.0000 | 0.0000 | 0.0000 | 0.0000 | 0.0000 | 0.0000 | 0.0000 | 0.0000 | 0.0000 | 0.0000 |
| **$Sb_2O_3$** | 4.3956 | 3.7544 | < LOD | < LOD | < LOD | < LOD | < LOD | < LOD | < LOD | < LOD | < LOD | < LOD |
| **Err** | 0.0225 | 0.0196 | 0.0000 | 0.0000 | 0.0000 | 0.0000 | 0.0000 | 0.0000 | 0.0000 | 0.0000 | 0.0000 | 0.0000 |
| **$As_2O$** | 0.0485 | 0.0243 | < LOD | < LOD | < LOD | < LOD | < LOD | < LOD | < LOD | < LOD | < LOD | < LOD |
| **Err** | 0.0014 | 0.0011 | 0.0000 | 0.0000 | 0.0000 | 0.0000 | 0.0000 | 0.0000 | 0.0000 | 0.0000 | 0.0000 | 0.0000 |
| **Cl** | 0.5837 | 0.7269 | 0.1515 | 0.1777 | 0.1268 | 0.1320 | 0.0836 | 0.0881 | 0.1282 | 0.0745 | 0.1050 | 0.0772 |
| **Err** | 0.0253 | 0.0283 | 0.0266 | 0.0243 | 0.0242 | 0.0251 | 0.0267 | 0.0257 | 0.0202 | 0.0213 | 0.0287 | 0.0279 |
| **Bi** | 0.0200 | < LOD | < LOD | < LOD | < LOD | < LOD | < LOD | < LOD | < LOD | < LOD | < LOD | < LOD |
| **Err** | 0.0025 | 0.0000 | 0.0000 | 0.0000 | 0.0000 | 0.0000 | 0.0000 | 0.0000 | 0.0000 | 0.0000 | 0.0000 | 0.0000 |

LOD – Limit of detection

**Tab. 1** – Continued.

| **Samples** | **PL25** | **PL26** | **PL27** | **PL28** | **PL29** | **PL30** | **PL31** | **PL32** |
|---|---|---|---|---|---|---|---|---|
| **color** | **bluish-green** | **red** | | | | | | |
| **Pigment** | **$Fe^{2+}$** | **Metallic Cu** | | | | | | |
| **MgO** | 7.8841 | 1.9044 | < LOD | < LOD | < LOD | < LOD | < LOD | < LOD |
| **Err** | 1.7030 | 1.7789 | 0.0000 | 0.0000 | 0.0000 | 0.0000 | 0.0000 | 0.0000 |
| **$Al_2O_3$** | 4.6794 | 1.1191 | 0.7857 | 1.0566 | 0.4236 | 0.8007 | 1.6037 | 1.0999 |
| **Err** | 0.4339 | 0.3753 | 0.3780 | 0.3757 | 0.3581 | 0.3544 | 0.3630 | 0.3690 |
| **$SiO_2$** | 61.6334 | 74.9558 | 76.4533 | 78.5251 | 70.4353 | 67.4367 | 72.7028 | 72.8470 |
| **Err** | 0.6170 | 0.6328 | 0.6316 | 0.6507 | 0.5749 | 0.5468 | 0.5959 | 0.5896 |
| **$P_2O_5$** | 2.1823 | 0.1634 | 0.1004 | 0.1989 | 0.1543 | 0.3063 | 0.2738 | 0.1965 |
| **Err** | 0.0761 | 0.0507 | 0.0510 | 0.0498 | 0.0511 | 0.0520 | 0.0506 | 0.0516 |
| **$SO_3$** | 0.8100 | 0.5340 | 0.6646 | 0.3028 | < LOD | 0.3873 | 0.1489 | < LOD |
| **Err** | 0.0135 | 0.0186 | 0.0194 | 0.0164 | 0.0269 | 0.0297 | 0.0239 | 0.0254 |
| **$K_2O$** | 6.0082 | 3.8836 | 3.9890 | 4.8817 | 2.2863 | 2.3137 | 2.5928 | 2.5954 |
| **Err** | 0.0378 | 0.0296 | 0.0297 | 0.0326 | 0.0230 | 0.0225 | 0.0242 | 0.0242 |
| **CaO** | 14.8698 | 9.5402 | 9.9190 | 8.6704 | 9.4445 | 10.3017 | 9.7854 | 10.1053 |
| **Err** | 0.0552 | 0.0429 | 0.0433 | 0.0409 | 0.0425 | 0.0435 | 0.0429 | 0.0433 |
| **FeO** | 1.4330 | 2.2586 | 2.2940 | 1.6913 | 3.0651 | 3.1550 | 2.6922 | 2.7713 |
| **Err** | 0.0120 | 0.0157 | 0.0156 | 0.0135 | 0.0152 | 0.0151 | 0.0145 | 0.0145 |
| **MnO** | 0.1649 | 0.7007 | 0.7052 | 0.6977 | 0.9396 | 0.9438 | 0.6357 | 0.6196 |
| **Err** | 0.0056 | 0.0113 | 0.0112 | 0.0112 | 0.0108 | 0.0106 | 0.0093 | 0.0090 |
| **$TiO_2$** | 0.2261 | 0.0891 | 0.0781 | 0.0669 | 0.0549 | 0.0878 | 0.0681 | 0.0456 |
| **Err** | 0.0059 | 0.0048 | 0.0049 | 0.0045 | 0.0052 | 0.0055 | 0.0049 | 0.0051 |
| **NiO** | 0.0014 | 0.0123 | 0.0131 | 0.0107 | 0.0203 | 0.0214 | 0.0130 | 0.0144 |
| **Err** | 0.0006 | 0.0018 | 0.0018 | 0.0015 | 0.0025 | 0.0025 | 0.0020 | 0.0021 |
| **CoO** | < LOD | < LOD | < LOD | < LOD | < LOD | < LOD | < LOD | < LOD |
| **Err** | 0.0000 | 0.0000 | 0.0000 | 0.0000 | 0.0000 | 0.0000 | 0.0000 | 0.0000 |
| **CuO** | 0.0091 | 3.5482 | 3.6827 | 2.9821 | 4.1978 | 4.2505 | 3.0358 | 3.0788 |
| **Err** | 0.0008 | 0.0130 | 0.0131 | 0.0113 | 0.0139 | 0.0137 | 0.0115 | 0.0118 |
| **PbO** | 0.0039 | 0.5107 | 0.5260 | 0.0773 | 3.2376 | 3.3879 | 2.7272 | 2.7993 |
| **Err** | 0.0012 | 0.0051 | 0.0051 | 0.0023 | 0.0126 | 0.0127 | 0.0110 | 0.0114 |
| **$SnO_2$** | < LOD | 0.0119 | < LOD | < LOD | 4.6269 | 5.4762 | 3.0791 | 3.0988 |
| **Err** | 0.0000 | 0.0065 | 0.0000 | 0.0000 | 0.0224 | 0.0254 | 0.0174 | 0.0177 |
| **$Sb_2O_3$** | < LOD | 0.0368 | 0.0400 | 0.0480 | 0.4309 | 0.4589 | 0.0383 | 0.0432 |
| **Err** | 0.0000 | 0.0056 | 0.0056 | 0.0053 | 0.0088 | 0.0089 | 0.0058 | 0.0060 |
| **$As_2O$** | < LOD | < LOD | < LOD | 0.0122 | < LOD | < LOD | < LOD | < LOD |
| **Err** | 0.0000 | 0.0000 | 0.0000 | 0.0012 | 0.0000 | 0.0000 | 0.0000 | 0.0000 |
| **Cl** | 0.0932 | 0.7311 | 0.7488 | 0.7785 | 0.6791 | 0.6656 | 0.6015 | 0.5979 |
| **Err** | 0.0289 | 0.0330 | 0.0327 | 0.0333 | 0.0313 | 0.0294 | 0.0316 | 0.0308 |
| **Bi** | < LOD | < LOD | < LOD | < LOD | < LOD | < LOD | < LOD | < LOD |
| **Err** | 0.0000 | 0.0000 | 0.0000 | 0.0000 | 0.0000 | 0.0000 | 0.0000 | 0.0000 |

LOD – Limit of detection

**Tab. 1** – Continued.

| **Sample** | **F1** | **F2** | **F3** | **F4** | **F5** | **F7** | **F8** | **F9** | **F10** |
|---|---|---|---|---|---|---|---|---|---|
| **Color** | **red** | **turquoise** | **turquoise** | **Light turquoise** | **dark blue** | **dark green** | **dark blue** | **black** | **Raw glass** |
| **Pigment** | **Metallic Cu** | | | | | | | **Mn** | **$Fe^{2+}$** |
| **MgO** | 1.8052 | < LOD | < LOD | < LOD | 2.2252 | < LOD | < LOD | 2.8847 | 4.5903 |
| **Err** | 1.9781 | 0.0000 | 0.0000 | 0.0000 | 1.7586 | 0.0000 | 0.0000 | 1.8724 | 1.6706 |
| **$Al_2O_3$** | 0.4957 | 0.6670 | < LOD | < LOD | 0.4906 | 0.7616 | 0.5010 | 2.7958 | 10.3910 |
| **Err** | 0.3664 | 0.3718 | 0.0000 | 0.0000 | 0.3569 | 0.3807 | 0.3783 | 0.4344 | 0.5462 |
| **$SiO_2$** | 53.400 | 77.9150 | 77.6051 | 62.2533 | 77.3650 | 71.2108 | 75.4625 | 67.2105 | 46.8749 |
| **Err** | 0.4992 | 0.6384 | 0.6374 | 0.4575 | 0.6433 | 0.6101 | 0.6405 | 0.6196 | 0.5480 |
| **$P_2O_5$** | 0.2830 | 0.1157 | 0.1701 | 0.1100 | 0.1617 | 0.1506 | 0.1459 | 0.4095 | 2.0407 |
| **Err** | 0.0555 | 0.0507 | 0.0514 | 0.0518 | 0.0501 | 0.0544 | 0.0531 | 0.0625 | 0.0874 |
| **$SO_3$** | < LOD | 0.4104 | 0.4225 | < LOD | 0.3744 | 0.1285 | 0.3433 | 0.2341 | 0.0809 |
| **Err** | 0.0773 | 0.0161 | 0.0158 | 0.0774 | 0.0156 | 0.0225 | 0.0152 | 0.0182 | 0.0073 |
| **$K_2O$** | 0.6288 | 4.4842 | 2.2055 | 1.6241 | 3.5693 | 3.5483 | 4.6064 | 2.8610 | 4.4872 |
| **Err** | 0.0172 | 0.0312 | 0.0233 | 0.0230 | 0.0284 | 0.0287 | 0.0322 | 0.0271 | 0.0346 |
| **CaO** | 2.4288 | 10.9662 | 11.5204 | 0.4108 | 9.9924 | 11.8379 | 13.0896 | 12.0604 | 30.1851 |
| **Err** | 0.0294 | 0.0458 | 0.0474 | 0.0283 | 0.0442 | 0.0484 | 0.0507 | 0.0497 | 0.0788 |
| **FeO** | 0.7259 | 0.8157 | 0.8733 | 0.1113 | 0.8166 | 1.2693 | 0.7653 | 1.9235 | 1.8088 |
| **Err** | 0.0104 | 0.0084 | 0.0088 | 0.0043 | 0.0085 | 0.0107 | 0.0084 | 0.0141 | 0.0151 |
| **MnO** | 0.1531 | 0.4956 | 0.4500 | < LOD | 0.3170 | 0.4334 | 0.2437 | 7.5819 | 0.2075 |
| **Err** | 0.0075 | 0.0083 | 0.0081 | 0.0045 | 0.0070 | 0.0082 | 0.0063 | 0.0312 | 0.0067 |
| **$TiO_2$** | 0.0328 | 0.1007 | 0.0978 | 0.0343 | 0.0865 | 0.1258 | 0.1076 | 0.1725 | 0.4573 |
| **Err** | 0.0055 | 0.0050 | 0.0052 | 0.0053 | 0.0049 | 0.0057 | 0.0053 | 0.0055 | 0.0088 |
| **NiO** | 0.0244 | 0.0820 | 0.0258 | 0.1140 | 0.1185 | 0.0236 | 0.0218 | 0.0058 | 0.0018 |
| **Err** | 0.0172 | 0.0020 | 0.0015 | 0.0143 | 0.0024 | 0.0022 | 0.0013 | 0.0011 | 0.0008 |
| **CoO** | 0.0109 | < LOD | < LOD | 0.0138 | 0.0997 | < LOD | 0.0982 | < LOD | < LOD |
| **Err** | 0.0017 | 0.0000 | 0.0000 | 0.0020 | 0.0011 | 0.0000 | 0.0011 | 0.0000 | 0.0000 |
| **CuO** | 7.3414 | 0.0449 | 1.4855 | 10.3658 | 0.1249 | 3.5397 | 0.0136 | 0.1993 | 0.0075 |
| **Err** | 0.0560 | 0.0014 | 0.0071 | 0.0489 | 0.0022 | 0.0130 | 0.0010 | 0.0032 | 0.0010 |
| **PbO** | 52.3915 | 0.0395 | 0.1614 | 33.3054 | 0.0677 | 2.4119 | 0.1239 | 0.9860 | < LOD |
| **Err** | 0.1661 | 0.0017 | 0.0015 | 0.1080 | 0.0020 | 0.0108 | 0.0025 | 0.0066 | 0.0000 |
| **$SnO_2$** | 0.5539 | < LOD | < LOD | 20.7159 | < LOD | 0.1614 | < LOD | 0.0169 | < LOD |
| **Err** | 0.0152 | 0.0000 | 0.0000 | 0.0779 | 0.0000 | 0.0071 | 0.0000 | 0.0058 | 0.0000 |
| **$Sb_2O_3$** | 0.1992 | 2.6976 | 4.1972 | 0.0000 | 2.9811 | 3.9314 | 3.8660 | 0.1428 | < LOD |
| **Err** | 0.0262 | 0.0134 | 0.0169 | 0.0217 | 0.0144 | 0.0199 | 0.0165 | 0.0060 | 0.0000 |
| **$As_2O$** | 1.0486 | 0.3853 | 0.1890 | 0.2322 | 0.5026 | < LOD | 0.0998 | < LOD | < LOD |
| **Err** | 0.0665 | 0.0025 | 0.0019 | 0.0377 | 0.0030 | 0.0000 | 0.0017 | 0.0000 | 0.0000 |
| **Cl** | 0.7418 | 0.6791 | 0.5633 | 0.6928 | 0.5772 | 0.4638 | 0.5862 | 0.5154 | 0.0847 |
| **Err** | 0.1084 | 0.0322 | 0.0313 | 0.0751 | 0.0319 | 0.0321 | 0.0322 | 0.0328 | 0.0286 |
| **Bi** | < LOD | 0.1009 | 0.0332 | < LOD | 0.2294 | < LOD | 0.3623 | < LOD | < LOD |
| **Err** | 0.0000 | 0.0023 | 0.0018 | 0.0000 | 0.0033 | 0.0000 | 0.0019 | 0.0000 | 0.0000 |

LOD – Limit of detection

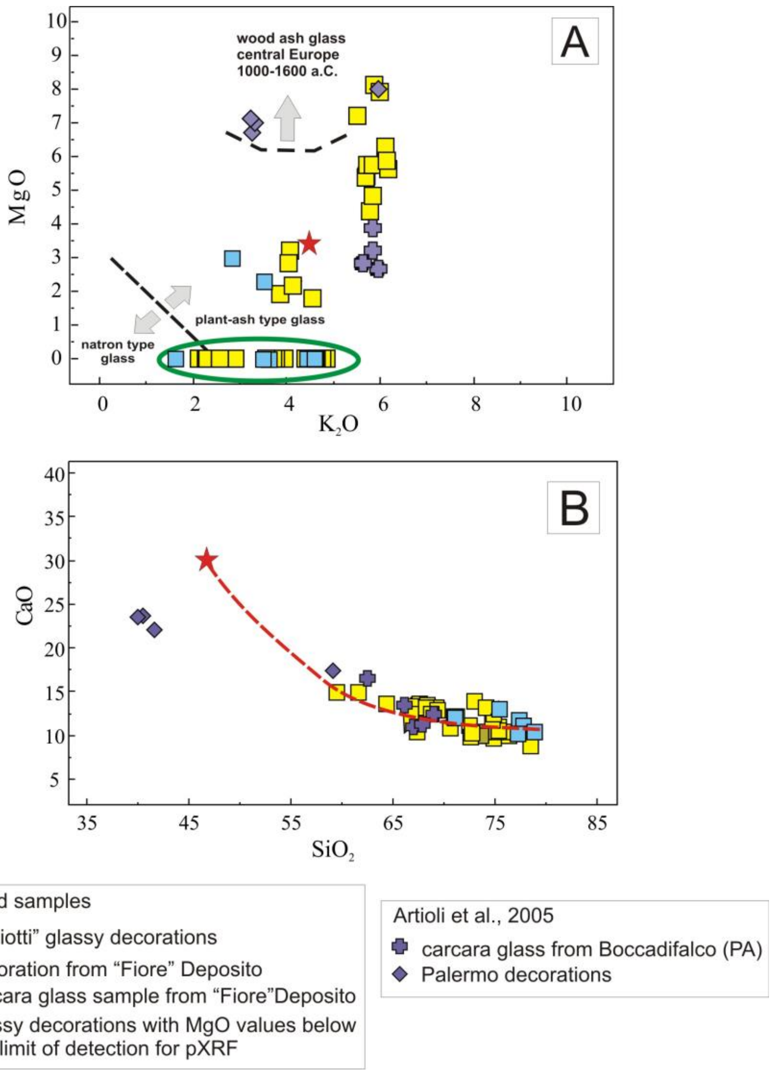

***Fig. 3 – a) $K_2O$ vs MgO classification diagram by Lilyquist and Brill (1995) indicates that different types of wood have been used during the firing process (Fig. 1); b) $SiO_2$ vs CaO variation diagram suggests the use of low pure limestone.***

On the contrary, data of the raw glass sample F10 indicate a composition made up of $SiO_2$ (~ 47 %), MgO (4.37 %), $K_2O$ (4.48 %), $Al_2O_3$ (10.39 %), FeO (1.8 %), and CaO (30.18 %). The minor oxides are present in very low amount, such as CuO (0.0075 %), or are under the limit of detection, such as PbO, $SnO_2$, $Sb_2O_3$ and CoO (Table 1, Appendix). Hence, the craftsmen used the carcara glassy waste retrieved from the lime kiln and suitably modified it, adding silica and/or other chemical substances, with the aim of obtaining the desired glass compositions for the production of the decorations.

Specifically, the composition of the raw glass sample is very similar to those of the bluish green samples (PL15-PL24), which show comparable high values of $P_2O_5$ and FeO (0.95-1.33 %) and very low amount of CuO (0.0180-0.0962 %). Probably, these bluish green glassy decorations were very little processed, in terms of the added elements, compared to the raw carcara glass.

Additional evidence in favor of the use of carcara glass as raw material comes from SEM and XRPD data. Inside the glass, perfectly rounded metal spherules of different sizes and up to 9 mm in diameter were seen during SEM-EDX analyses (Fig. 4A, B, C). Among the analysed metal spherules, schreibersite [$(Fe,Ni)_3P$] was found (Fig. 4d). In most of the XRPD patterns (e.g. Fig. 4E), the presence of the mineral phase schreibersite was detected, in particular, in the blue glassy decorations. Schreibersite is generally a very rare iron nickel phosphide mineral, though common in iron-nickel meteorites. Its presence undoubtedly proves the occurrence of reducing conditions during the production process, from which derive glass used to realize the studied decorations. The forming environment of schreibersite is compatible with the extremely reducing conditions of CaO-producing furnace. The P reacted with Fe during the glass formation to yield unmixed droplets of Fe phosphides that were visible in the SEM backscattered electron maps, both in the slags and in the decoration glass samples, and indicate a highly reducing atmosphere as already suggested in a previous study (Artioli et al. 2009).

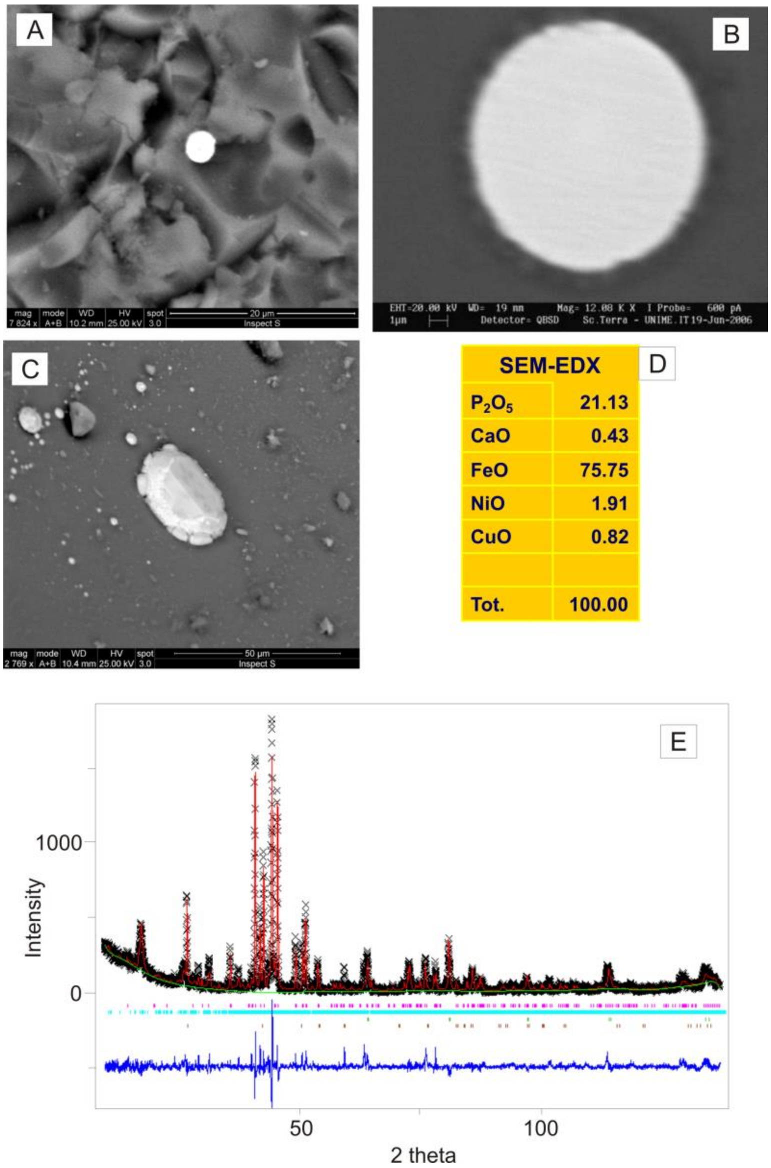

| SEM-EDX | |
|---|---|
| $P_2O_5$ | 21.13 |
| CaO | 0.43 |
| FeO | 75.75 |
| NiO | 1.91 |
| CuO | 0.82 |
| | |
| Tot. | 100.00 |

*Fig. 4 – Schreibersite particles and composition. A) rounded particle of schreibersite in blue glass decoration and B) magnification of a rounded particle of schreibersite; c) heuedral crystal of schreibersite in carcara glass, D) semi-quantitative SEM-EDX analysis of schreibersite particles; E) Qualitative Rietveld XRPD pattern performed on extracted particles of schreibersite .*

## 3.2 PIGMENTS AND OPACIFIERS

Turquoise and blue decorations – The nuances vary from turquoise and light turquoise to dark blue and bluish-green. Specifically, the light turquoise color can be ascribed to the presence of high copper contents, occurring in the form of $Cu^{2+}$ cations (e.g. Arletti et al. 2006a, b), and/or to the natural color of the raw carcara glass determined by $Fe^{2+}$ cations (Artioli et al. 2009). In particular, the samples, PL9 - PL13 (CuO=2.1905 ÷ 3.8956 %) and F4 (CuO=10.34 %), contain the highest amounts of CuO (Tab. 1). Turqouise and dark blue decorations are characterized by very low amount of Cu (0.012 - 0.057 %), and the contribution of $Fe^{2+}$ is probably important. With respect to the turquoise and dark blue samples, the nuances of the blue tesserae could have been as a result of cobalt (CoO=0.017 - 0.077 %) (Tab. 1). The bluish-green decorations reflect the color of the raw carcara glass, since they are very similar to it in terms of major oxides composition (see previous paragraph) and show very low copper content (CuO=0.0071-0962 ppm).

SEM-BSE observations indicate the presence in the glass matrix of minute (3–4 µm) frequently aggregated euhedral Sb, Ca-rich crystals (Fig. 5A, B, C and d and Table 1), demonstrating that the opaque effects of these decorations could be ascribed to Ca-antimonate ($Ca_2Sb_2O_7$), a well-known white opacifier widely used in ancient times (e.g. Shortland 2002; Shortland and Eremin 2006; Di Bella et al. 2014).

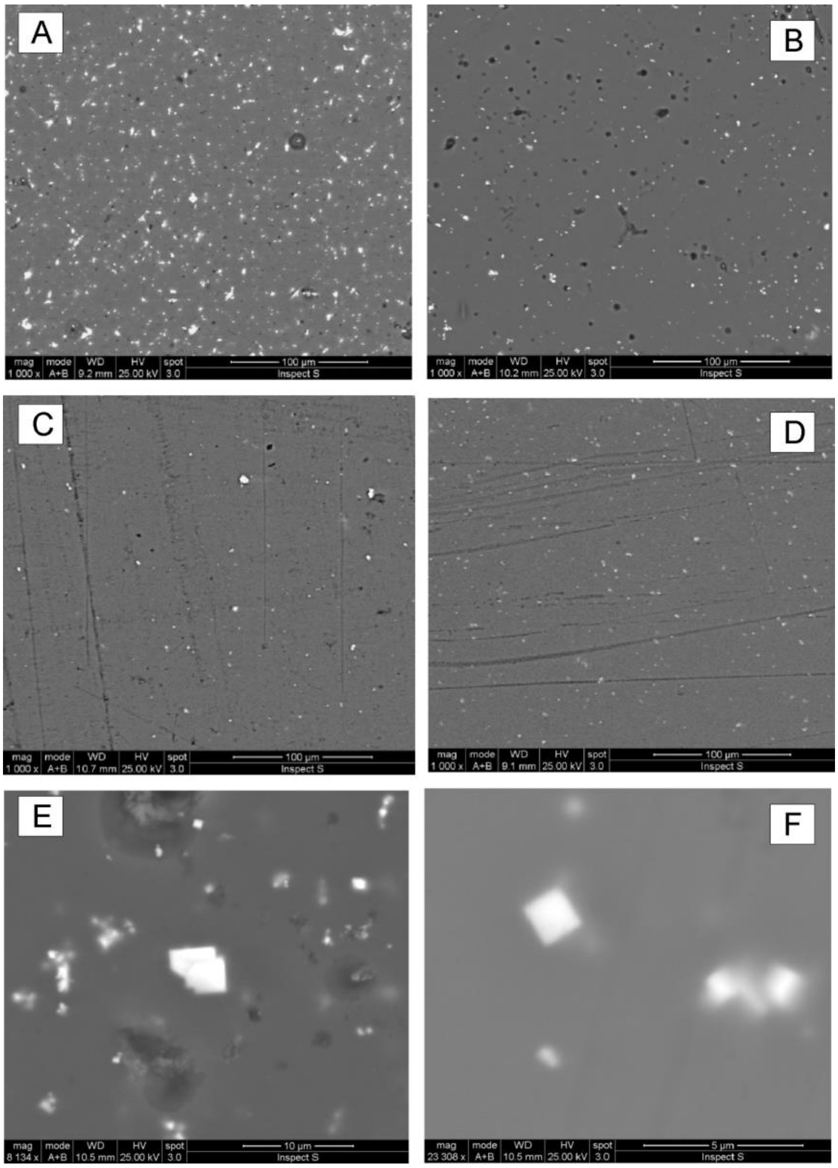

***Fig. 5 - SEM-BSE images of the studied glassy decorations characterized by blue nuances: a) light turquoise glass; b) turquoise c) dark blue glass; d) bluish-green glass; e) Ca-antimonate in turquoise, and f) bluish green glasses.***

Ca-antimonate crystals are perfectly euhedral (Fig. 5E, F), suggesting that in these decorations the white opacifier was produced in situ by adding Sb-containing raw materials to the glass melt (Di Bella et al. 2014). Detailed XRPD analyses of the glass samples allowed precise identification of the ortho-rhombic Ca-antimonate (PDF number 26-0293). On the XRPD pattern reported in figure 6, the observed peaks are those known in literature for Ca-antimonate phase (Arletti et al., 2006). These peaks overlap with the typical background caused by the amorphous silicate matrix.

A previous study on the blue decorations of the Baroque glass used to decorate altars of several churches of Palermo was carried out by Artioli et al. (2009). The result of the study excluded Co and Cu as colouring agents for their very low or undetected concentrations, and suggested the contribution of iron in divalent form and octahedral coordination as a colouring agent. Our results, however, show that Co, Cu and Fe all contribute to the blue nuances of the glassy decorations from the Messina Museum. These differences could be interpreted as being the result of different recipes or methods locally used in

Sicily by the craftsmen to obtain blue nuances from an original carcara raw material.

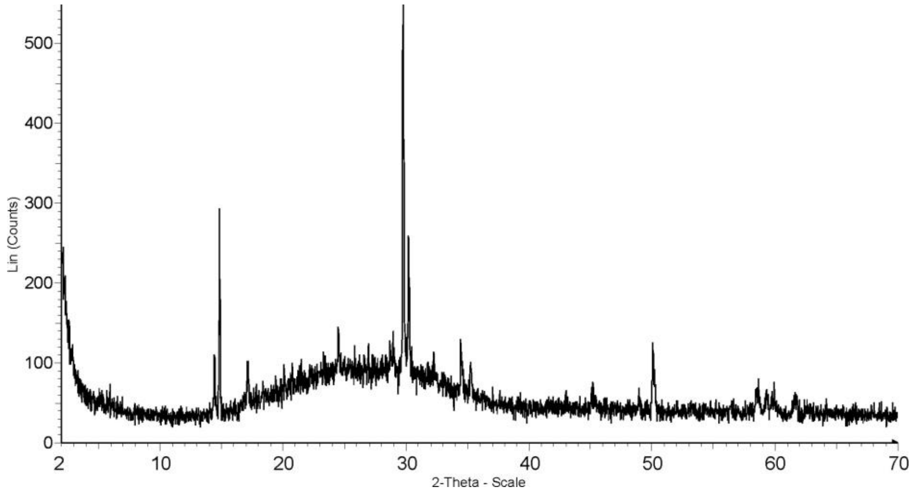

*Fig. 6 – XRPD pattern of Ca-antimonate.*

Opaque red decorations – SEM observation of the red glassy decorations F1 and PL26÷32 exhibited textures (Fig. 2A), depending on the different distributions of the sub-micrometer clusters of metallic copper widely dispersed in the glass matrix. This feature influenced also the color of the several red nuances. The clusters are almost visible in Fig. 7A-B and, as confirmed by numerous previous investigations (see for example Arletti et al. 2006a-b, and references herein cited; Sabatino 2007; Di Bella et al. 2014), are the origin of both opacity and the red color. The small size of the Cu clusters made it impossible to accurately avoid the effects of the surrounding glass composition on the chemical analyses reported in Table 1. SEM back-scattered electron images (BSE) revealed cluster dimensions < 200 nm (Fig. 7A, B). Moreover, a detailed observation of the clusters revealed the typical rounded morphology of metallic copper clusters. The nature of the clusters was also confirmed by the diffraction patterns, which displayed the reflections of metallic copper (Fig. 7A, B). In addition to the high copper content, the red tesserae are also characterized by high concentrations of iron, lead, tin, and phosphorus (Tab. 1).

From a chemical point of view, all the analysed red samples are relatively heterogeneous (Tab. 1). Specifically, XRF data reveal that the composition of F1 red glass (Tab. 1) is particularly rich in Pb (PbO 52.39 %), with high CuO (7.34 %) and low SnO (0.55 %), whereas the PL red samples, despite their comparable copper content (CuO from about 3.08 to 5.45 %), show variable SnO and PbO contents (Tab. 1). In particular, PL26, PL27 and PL28 (brown-red color with metallic luster, Fig. 1e) are characterized by lower amounts of SnO (≤ 0.0019 %) and PbO (0.007-0.526 %), whereas PL29÷32 group (fire red with slight metallic luster, Fig. 1f) show highest values of SnO (3.07-5.47 %) and PbO (2.72 – 3.38 %). Detailed XRPD analyses of these red samples allowed precise identification of the SnO (cassiterite; PDF number 041-1445) phase. The particularly high SnO and PbO content suggests the deliberate addition of Sn- and Pb-containing materials to the melt, with the aim of preventing copper oxidation. Previous studies evidenced the use of cassiterite as an opacifier in decoration works (Panagopoulou et al., 2018).

Therefore, the craftsmen added suitable elements or oxides to the processed carcara glass with the aim of obtaining the desired nuances.

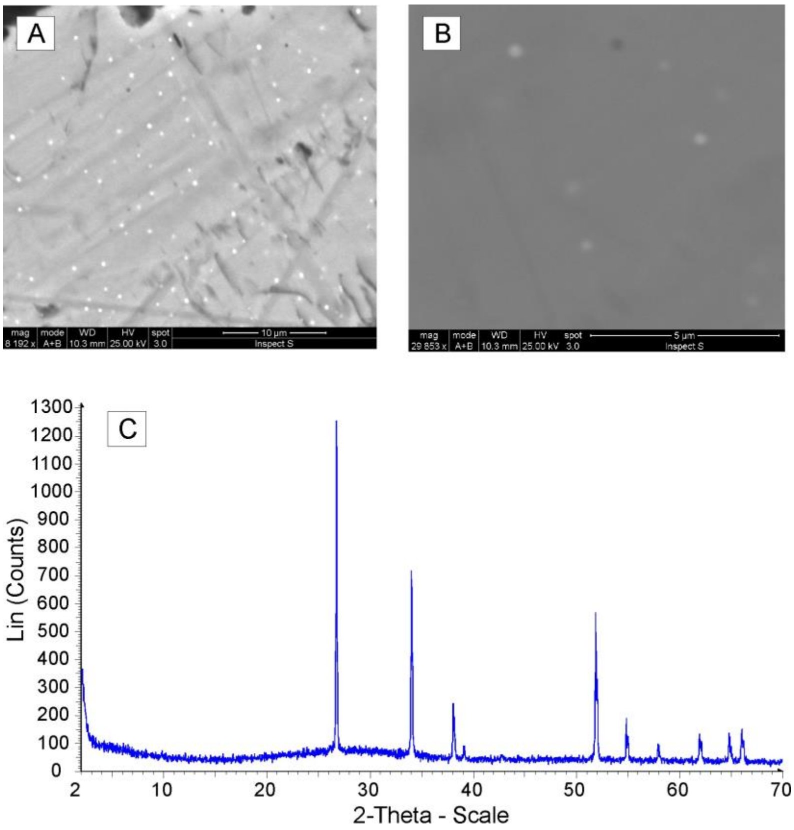

*Fig. 7 - SEM-BSE representative images of the studied red glassy decorations. a) main texture; b) Cu nano-clusters in red glass; C) XRPD pattern of SnO.*

## 4. CONCLUSIONS

Chemical XRF data obtained by means of non-destructive analyses of the Baroque glassy decorations indicate that the used raw material is compositionally homogeneous and belongs to the so-called plant ash to wood ash glass types.

The chromophore species identified in the transparent and translucent tesserae — and deduced by comparison with spectroscopic studies in the literature — are 1) $Cu^{2+}$ cations dispersed in the glass matrix of the light turquoise glass; 2) $Fe^{2+}$ and Co, with very low Cu, in turquoise and dark blue glasses; 3) high values of Cu in red glass.

SEM and X-ray diffraction investigations of the opaque tesserae allowed the identification of opacifier phases, such as 1) metallic CuO, which form clusters of different dimensions inside the red tesserae; 2) both the hexagonal $CaSb_2O_6$ and the orthorhombic $Ca_2Sb_2O_7$ calcium antimonate phases in the opaque pale blue, turquoise, and white tesserae.

## REFERENCES

Abbate, F. (1997) Storia dell'arte nell'Italia meridionale: il secolo d'oro. Donzelli editore, pp. 1-131.

Accascina, M. (1963) A Messina i mischi, trabischi, rabischi, *Antichità viva*, 2, pp. 9-10.

Arletti, R., Ciarallo, A., Quartieri, S., Sabatino, G. and Vezzalini, G. (2006a) Archaeometric analyses of game counters from Pompeii. In: Maggetti, M., Messiga, B. (eds) *Geomaterials in Cultural Heritage*, Vol. 257, pp. 175–186. Geological Geological Society of London (UK), London.

Arletti, R., Quartieri, S. and Vezzalini, G. (2006b) Glass mosaic tesserae from Pompeii: an archaeometric al investigation, *Periodico di Mineralogia*, Vol. 76, pp. 25–38.

Artioli, G., Nicola, C., Montana, G., Angelini, I., Nodari, L. and Russo, U. (2009) The blue enamels in the baroque decorations of the churches of Palermo, Sicily: $Fe^{2+}$-coloured glasses from lime kilns, *Archaeometry*, vol. 51, No. 2, pp. 197–213.

Balenzano, F. and Moresi, M. (2004) Scorie vetrose da fornaci per la produzione artigianale Di calce viva (Minervino Murge - Bari), *Atti della Società Toscana di Scienze Naturali*, serie A, Vol. 109, pp. 57-68.

Di Bella, M., Quartieri, S., Sabatino, G., Santalucia, F. and Triscari, M. (2014) The glass mosaics tesserae of "Villa del Casale" (Piazza Armerina, Italy): a multi-technique archaeometric study, *Archaeological and Anthropoogical Sciences*, Vol. 6, No, 4, pp. 345-362.

Giuffrè, M. (1992) I marmi mischi delle chiese di Palermo. Palermo: Sellerio.

Hills, H., 1999. Marmi Mischi Siciliani: Invenzione e Identità (Inlaid polychromatic marble decoration in early modern Sicily: Invention and identity), *Società Messinese di Storia Patria*, Scholarly monograph series, Messina, 1999. 457 pp.

Liritzis, I, Laskaris, N, Vafiadou A, Karapanagiotis I, Volonakis, P, Papageorgopoulou, C, Bratitsi, M (2020) Archaeometry: an overview. *SCIENTIFIC CULTURE*, Vol. 6, No. 1, pp. 49-98 DOI: 10.5281/zenodo.362522.0

Lilyquist, C. and Brill, R.H. (1995) Studies in ancient Egyptian glass, Metropolitan Museum of Art, New York

Mongitore, A., (1742) Della Sicilia ricercata nelle sue cose più memorabili, Palermo.

Montana, G. and Gagliardo Briuccia, V. (1998) I marmi ed i diaspri del Barocco siciliano, S.F. Flaccovio editore, Palermo, 127 pp.

Napoleone, C. (2001) L'impiego dei diaspri e delle agate di Sicilia dal XVI al XVII secolo. In Splendori di Sicilia. Arti Decorative dal Rinascimento al Barocco., pp. 192-203, Ed. Charta.

Panagopoulou, A., Lampakis, D., Christophilos, D., Beltsios, K., Ganetsos, Th. (2018) Technological examination of Iznik ceramics by SEM-EDX, Raman, XRD, PLM: a case study. *Scientific Culture*, Vol. 4, No. 3, pp. 27-33

Pavone Alajmo, M.P. (2001) Mischi, rabischi e tra mischi: tarsie marmoree policrome del Museo Regionale di Messina. In Splendori di Sicilia. Arti Decorative dal Rinascimento al Barocco, pp. 184-191. Ed. Charta,

Piazza, S. (2007) I colori del Barocco: architettura e decorazione in marmi policromi nella Sicilia del Seicento. Palermo: Flaccovio.

Pouchou, J.L. and Pichoir, L. (1984) Possibilités d'analyse en profondeur à la microsonde électronique. *Journal of Microscopic Spectroscopy Electron*, Vol. 9, pp. 99–100.

Pouchou, J.L. and Pichoir, L. (1985) Les elements très legers en microanalyse X – Possibilités des modèles récents de quantify cation, *Journal of Microscopic Spectroscopy Electron*, Vol. 11, pp. 229–250.

Sabatino G (2007) Vetri archeologici di età romana (dal II sec. a.C. al VI sec. d.C.) in Sicilia: attribuzione di provenienza e caratterizzazione delle tecniche costruttive. PhD thesis, Università di Messina

Schiavo, D. (1756) Descrizione di alcune produzioni naturali della Sicilia, Venezia.

Shannon, R.F. (2012) Bruker AXS Handled, Inc. United State Patent n. US 8.223.925 B2, July 17, pp. 13.

Shortland, A.J. (2002) The use and origin of antimonate colorants in early Egyptian glass, *Archaeometry*, Vol. 44, pp. 517–31.

Shortland, A.J. and Eremin, K. (2006) The analysis of second millennium glass from Egypt and Mesopotamia, part 1: new WDS analyses, *Archaeometry*, Vol. 48, No 4, pp. 581–603.

Sola, V. (2015) Baroque Decoration: the Marble Inlays. Palermo: Regione siciliana, Assessorato dei beni culturali e dell'identità siciliana, Dipartimento dei beni culturali e dell'identità siciliana.